

phys. stat. sol. (a) **175**, 23 (1999)

Subject classification: 78.20.Bh; 78.66.Db; S5.11; S5.12

## Optical Properties of Germanium Nanocrystals

M. PALUMMO, G. ONIDA, and R. DEL SOLE

*Istituto Nazionale per la Fisica della Materia, Dipartimento di Fisica dell' Università di Roma "Tor Vergata", Via della Ricerca Scientifica, I-00133 Roma, Italy*

(Received May 8, 1999)

We study the electronic structure and the optical properties of germanium clusters up to about  $10^3$  atoms, by using a semi-empirical tight-binding approach. Germanium nanocrystals are related to quantum dots growing, by a self-organization process, in sapphire matrices. The optical properties of such dots are experimentally found to be strongly influenced by quantum confinement effects. We investigate these effects from the theoretical point of view, calculating the optical spectra in the single-particle approximation. Inclusion of the electron-hole interaction is found to yield visible effects.

### 1. Introduction

During the last few years semiconductor quantum dots received much attention because of their potential technological applications, and their importance in understanding the physics of zero-dimensional structures. A considerable amount of work has been devoted to the study of self-organized quantum dots in III-V and II-VI semiconductor systems, and more recently in the homopolar semiconductors like Si and Ge.

The visible photoluminescence observed in silicon and more recently in germanium nanocrystals [1,2] attracted much attention both from the fundamental point of view and for the possible applications to optical devices. Peng et al. [3] showed, from photoluminescence measurements, that an indirect to direct conversion occurs in Ge quantum dots. Moreover, confinement effects are observed in the vibrational spectra of germanium nanoparticles [4, 5]. Less literature is present on the optical absorption spectra.

Absorption measurements, as a function of the size reduction, were obtained recently by Tognini et al. [6] for quantum dots of germanium grown by the evaporation-condensation self-organization technique in an amorphous  $\text{Al}_2\text{O}_3$  matrix. This growth method permits to minimize the stress and the matrix perturbation, and provides a relatively narrow size distribution. The nanoparticles obtained with this technique have the shape of truncated spheres and are single crystals, with extremely varying size, typically from ten to a few thousand Å. The experimental absorption spectra, obtained by subtracting from the overall measured spectra the absorption of the matrix, show a relevant blue-shift of the  $E_2$  peak and a weakening of the  $E_1$  peak, as a function of size reduction. The different behaviours of the two peaks is qualitatively interpreted by the authors of ref. [6] in terms of quantum confinement, and in connection with the different nature of the two structures.

From the theoretical point of view, the quantum confinement effect on the onset of the absorption spectra has been studied in the case of silicon dots [7, 8]. Full optical absorption spectra have been calculated by Wang and Zunger [9] for the same system.

No similar calculation is available in the case of germanium. Hence, in the present paper, we study the optical absorption spectra of Ge quantum dots and compare them with the available experimental data.

## 2. Calculation and Results

The spherical dots are modelled generating the atomic positions at the bulk interatomic distances up to a maximum radius. The external atoms are replaced by hydrogen atoms, in order to saturate all the Ge dangling bonds.

For comparison, we also computed some optical spectra without saturating the Ge atoms in the external positions. The differences will be shown in the following.

As a first step, we calculate the one-electron states of the germanium nanocrystals. The calculations are performed using the semi-empirical tight-binding Hamiltonian described in ref. [10], with a five-orbital per atom basis set ( $sp^3s^*$ ). The matrix elements of the momentum operator between atomic orbitals, needed to evaluate the optical properties, are computed according to

$$\mathbf{p} = i \frac{m}{\hbar} [H, \mathbf{r}] \quad (1)$$

and expanding the commutator on the (approximately) complete ( $sp^3s^*$ ) basis set. Only intra-atomic matrix elements of  $\mathbf{r}$  are retained. For the intra-atomic dipole matrix elements we use  $\langle s | x | p_x \rangle = 0.2 \text{ \AA}$  and  $\langle s^* | x | p_x \rangle = 1 \text{ \AA}$ , successfully used elsewhere [11]. Before performing the calculations for the spherical dots, the electronic structure of bulk germanium has been checked against the original work of Vogl et al. [10].

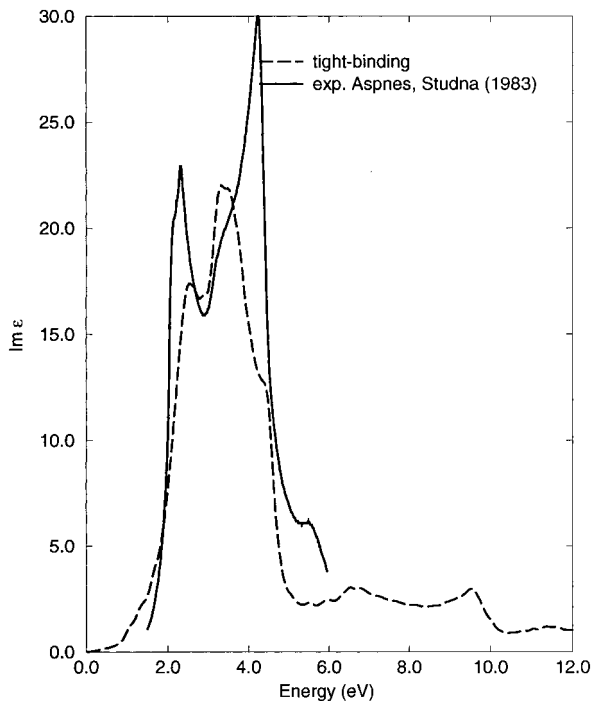


Fig. 1. Comparison between the bulk Ge theoretical optical spectrum (dashed line) obtained within the one-particle tight-binding approach and the experimental spectrum obtained by ellipsometry (full line) from ref. [12]

Using the Fermi golden rule, the imaginary part of the bulk dielectric function is obtained through the one-particle tight-binding eigenvectors and eigenvalues, and using 825  $k$ -points in the irreducible wedge of the Brillouin zone. A comparison with the experimental results of Aspnes and Studna [12] is shown in Fig. 1. The position of the low energy peak  $E_1$  is just slightly overestimated (2.5 eV instead of 2.2 eV) while its intensity is underestimated. Both the effects can be explained by neglecting the excitonic effect in the calculation of the optical spectrum. Moreover, the experimental curve shows a well pronounced peak  $E_2$  at 4.26 eV and a shoulder at 3.5 eV, while in the theoretical spectrum the situation is reversed: a large peak at 3.5 eV is present, while the structure at 4.26 eV appears just as a shoulder. This can be attributed to the limits of the  $sps^*$  first-neighbours tight-binding parametrization which fails to describe correctly the dispersion of the second conduction band, along the X-K direction [10]. The  $E_1$  peak is due essentially to transitions along the  $\Gamma$ -L direction, while the  $E_2$  peak appears to arise from a well defined, limited region inside the Brillouin zone. This region is near the Chadi Cohen special point  $2\pi/a (3/4, 1/4, 1/4)$ . The shoulder at 3.3 eV in the experimental spectrum is instead due to transitions from the last occupied state in  $\Gamma$  to the second unoccupied state near  $\Gamma$  ( $\Gamma'_{15} \rightarrow \Gamma'_2$ ).

The imaginary parts of the dielectric functions of the nanocrystals are calculated following the same approach used for the bulk, but using the dot volume to normalize the result. The  $\epsilon_2(\omega)$  of four spherical dots ( $\text{Ge}_{87}\text{H}_{76}$ ,  $\text{Ge}_{167}\text{H}_{124}$ ,  $\text{Ge}_{293}\text{H}_{172}$  and  $\text{Ge}_{633}\text{H}_{300}$  with radii of 8, 10, 12, 15 Å, respectively) are shown in Fig. 2. The structures appearing at about 6 eV are essentially due to the presence of the surface hydrogens. A blue-shift of the spectra due to the quantum size effect is present, together with a reduction of the intensity of the two main bulk structures.

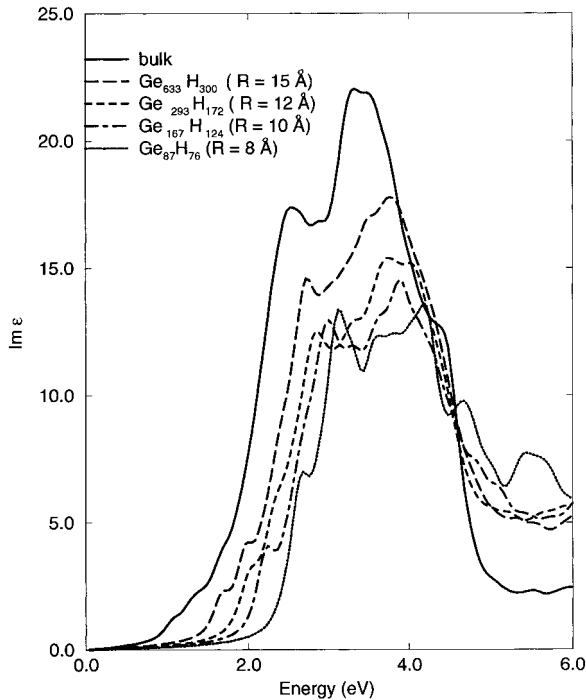


Fig. 2. The one-particle theoretical spectra, obtained for four different dots, are compared with the spectrum of bulk germanium. In all the cases shown the surface dangling bonds are saturated with hydrogen atoms

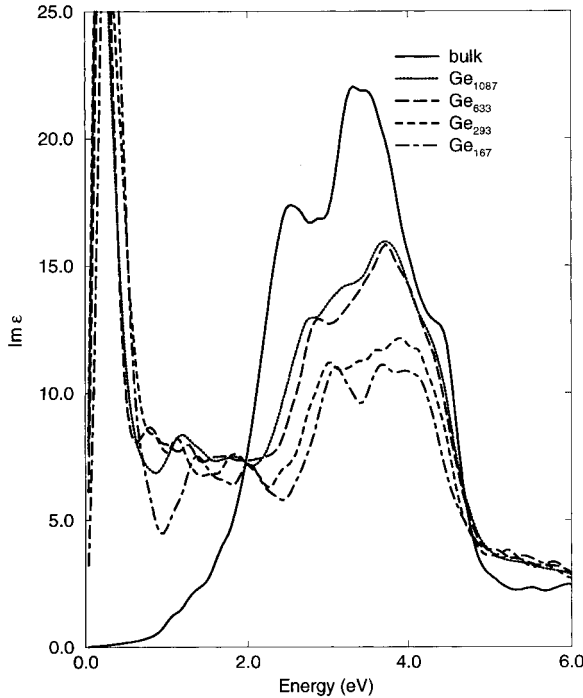


Fig. 3. One-particle theoretical optical spectra obtained for four different dots compared with the spectrum of bulk germanium. In all the four cases shown here, only Ge atoms are used, then the surface states are present

The size scaling of the band gap is compatible with the law  $\Delta E_g(R) = R^{-\alpha}$  with  $\alpha = 0.8$ . An exponent lower than 2, which is the value predicted by simple particle-in-a-box effective mass models, has also been found, in the silicon dots, by ab-initio calculations of Wang and Zunger [9].

Fig. 3 shows  $\epsilon_2(\omega)$  obtained for four different bare Ge dots (no H at the surface). In this case, a first low energy peak (due to the presence of surface states) occurs. Only little differences show up between the spectra of the two large dots (633 and 1087 Ge atoms), and between the two dots with 167 and 293 atoms. In both figures (Figs. 2 and 3) the  $\epsilon_2(\omega)$  of the bulk case is plotted for comparison.

For the dots with  $R = 8$  and  $12 \text{ \AA}$ , we repeated the  $\epsilon_2(\omega)$  calculations considering Si instead of Ge, in order to see the differences. Fig. 4 shows the optical absorption spectra for the two silicon dots.

Finally, Fig. 5 shows the comparison of our single-particle optical spectra with the experimental results of ref. [6], for the  $R = 12$  and  $15 \text{ \AA}$  germanium dots. The position of the theoretical peaks are clearly blue-shifted with respect to their bulk positions. The theoretical  $E_1$  shift is  $0.3 \text{ eV}$  for  $R = 12 \text{ \AA}$  and  $0.2 \text{ eV}$  for  $R = 15 \text{ \AA}$ . However, in the experimental curves the  $E_1$  structure does not display any evident blue-shift, but only an intensity decrease.

In order to look for the reason of this quantitative disagreement between the theoretical spectra and the experiments we included excitonic effects. The first step is to calculate them perturbatively [8]. The energy differences between valence and conduction bands in the  $\epsilon_2(\omega)$  formula are calculated including the electron-hole Coulomb attraction as described in the following.

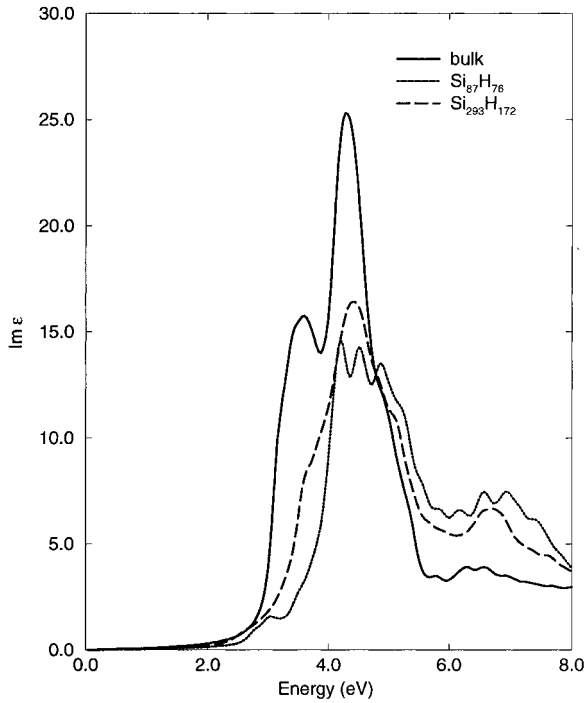


Fig. 4. Results for the optical spectra of silicon dots, compared with the bulk spectrum, computed within the present tight-binding one-particle approach

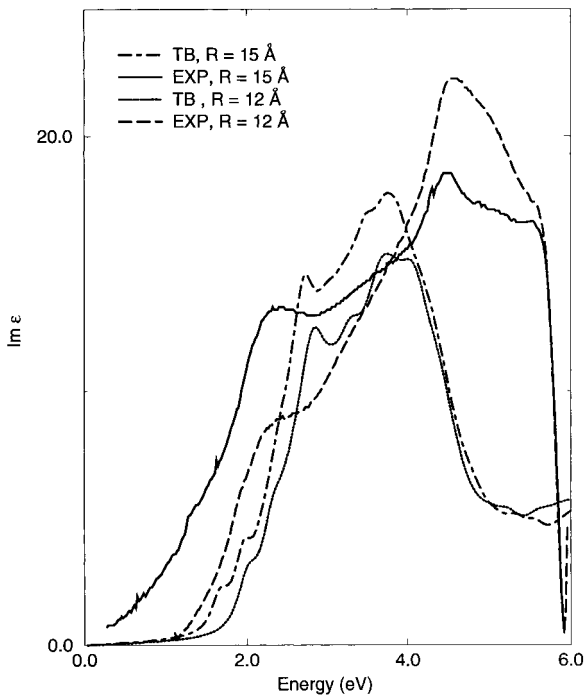


Fig. 5. Comparison between the one-particle theoretical optical spectra and experimental results from ref. [6] for the Ge dots

The Coulomb terms, given by

$$\left\langle \psi_i^c(r_e) \psi_j^v \left( (r_h) \left| \frac{e^2}{\epsilon|r_e - r_h|} \right| \psi_i^c(r_e) \psi_j^v \right) (r_h) \right\rangle \quad (2)$$

can be evaluated expanding the one-particle wave functions in terms of the atomic orbitals of the tight-basis  $\psi = \sum_a c_a \phi_a$ , where  $a$  is the index of the atomic orbitals.

We obtain a sum of terms such as

$$V_{a,b}^{d,b'} = \left\langle \phi_a(r_e) \phi_b(r_h) \left| \frac{e^2}{\epsilon|r_e - r_h|} \right| \phi_{a'}(r_e) \phi_{b'}(r_h) \right\rangle. \quad (3)$$

Coherently with what we have done in calculating the one-particle states, we neglect the overlaps, obtaining

$$V_{a,b}^{d,b'} = \delta_{a,a'} \delta_{b,b'} \int \frac{|\phi_a(r_e)|^2 |\phi_b(r_h)|^2 e^2}{\epsilon|r_e - r_h|} d^3 r_e d^3 r_h. \quad (4)$$

As the atomic orbitals are by definition strongly localized on the atoms, we approximate  $|r_e - r_h|$  by its value at the positions  $R_a$  and  $R_b$  of the atoms with respective functions  $\phi_a$  and  $\phi_b$ .

The final expression is

$$V_{a,b}^{d,b'} = \delta_{a,a'} \delta_{b,b'} \frac{e^2}{\epsilon|R_a - R_b|}. \quad (5)$$

This expression is no longer valid when  $R_a$  and  $R_b$  are equal. In this case the term  $V_{a,b}^{d,b'}$  is the Coulomb energy between two electrons on the same atom. For the dielectric function  $\epsilon$  appearing in the formula we used the parametrization proposed by Cappellini et al. [13], which was obtained for the bulk and which includes the  $|r - r'|$  dependence.

In reciprocal space it is given by

$$\epsilon(q) = 1 + \frac{1}{\frac{1}{\epsilon_0 - 1} + \alpha \frac{q^2}{q_{\text{TF}}^2} + \frac{\hbar^2 q^4}{4m^2 \omega_p^2}}, \quad (6)$$

where  $q_{\text{TF}} = \left( \frac{4}{\pi} k_F \right)^{1/2}$  and  $\omega_p = \left( \frac{4\pi Qe}{m} \right)^{1/2}$ .

Then the intra-atomic Coulomb integrals ( $U_{ii}$ , we neglect the off-diagonal integrals) are calculated using the Fourier transform of the screened Coulomb potential.

For the atomic wave functions  $\phi_s$  we used the parametrizations proposed in ref. [15] and used also in reference [16],

$$\phi_p(r) = N_p \mathbf{r}_p r e^{-\frac{r}{2r_p}}, \quad (7)$$

where  $\mathbf{r}_p$  means  $\mathbf{r}_+ = x + iy$ ,  $\mathbf{r}_- = x - iy$  and  $\mathbf{r}_0 = z$

$$\phi_s(r) = N_s r e^{-\frac{r}{2r_s}}. \quad (8)$$

Here  $N_p$  and  $N_s$  are the normalization constants, and  $r_s$  and  $r_p$  are 0.43 and 0.48 a.u., respectively.

We obtain  $U_{s,s} = 3.22$  eV,  $U_{p_1,p_1} = 1.22$  eV,  $U_{s,p} = 1.79$ . So far we have not calculated  $U_{s^*,s^*}$ , putting it equal to zero.

We find no relevant differences in the final spectrum if we put  $U_{s^*,s^*} = U_{s,s}$  and also if we use the Coulomb integrals obtained using the electron wave functions of an atomic DFT-LDA calculation.

The effect of the inclusion of the Coulomb interactions for the dots with  $R = 12$  and  $15$  Å is shown in Fig. 6.

Fig. 7 shows the spectra (for the dot with  $R = 8$  Å) obtained in the one-particle scheme and with the inclusion of the electron–hole interaction both for the silicon and germanium case. The red-shift due to the Coulomb–hole attraction can qualitatively explain the experimental features of ref. [6] where no shift of the  $E_1$  structure was seen, but the perturbative approach is insufficient to eliminate the discrepancy. This hypothesis is substantiated also by previous calculations on silicon dots performed by

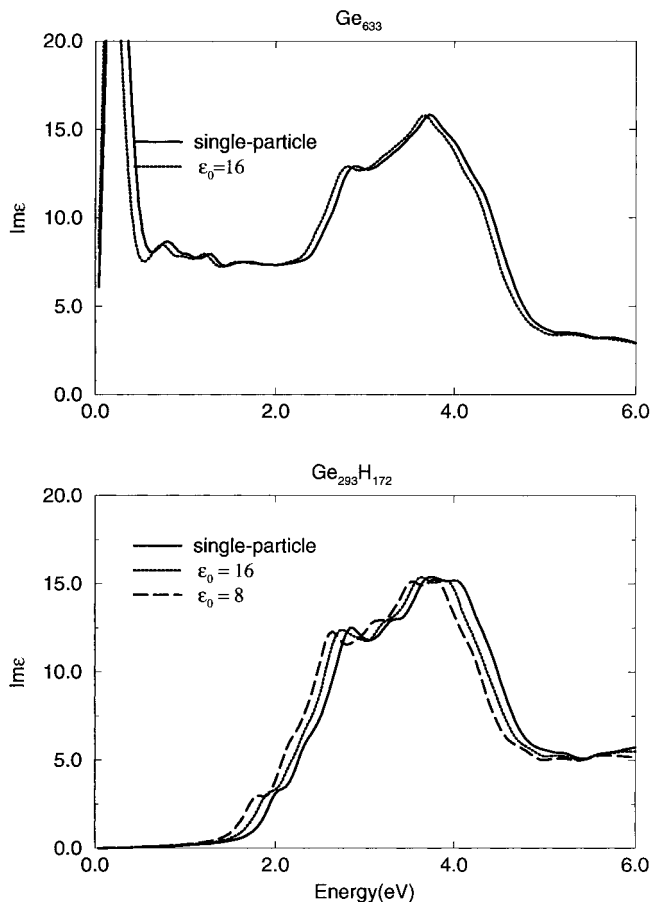


Fig. 6. Theoretical optical spectra obtained including the diagonal electron–hole interaction as discussed in the text, compared with the one-particle results for a typical pure Ge dot ( $\text{Ge}_{633}$ ) and for a saturated one ( $\text{Ge}_{293}\text{H}_{172}$ )

Hill and Whaley [14], who performed a two-particle tight-binding calculation in silicon dots and shown that the single-particle band-edge eigenfunctions are no good approximations to the exciton wave functions. We note also that the red-shift decreases with increasing dot size.

Moreover, it is important to underline that it is not obvious which value for the screening function is better to use in the electron-hole integrals. In fact, previous works for silicon dots indicate a reduction of the screening as the dot size  $R$  diminishes [9]. For this reason we calculated the optical spectrum also using in the Coulomb-hole attraction a value of  $\epsilon = 8$  (obtained by scaling the value calculated by Wang and Zunger in a silicon dot of radius about 10 Å, to the germanium case). For this reason in Fig. 7 (and in the second part of Fig. 6) we report curves obtained with different values of the dielectric constant. The reduction of the screening to the reasonable value of  $\epsilon = 8$  is again not enough to resolve the discrepancy to the experimental results; we tried also to calculate the spectrum with a lower value of the dielectric constant  $\epsilon = 2$ . In this case the red-shift is clearly more pronounced but we believe that so small values of  $\epsilon$  are not realistic.

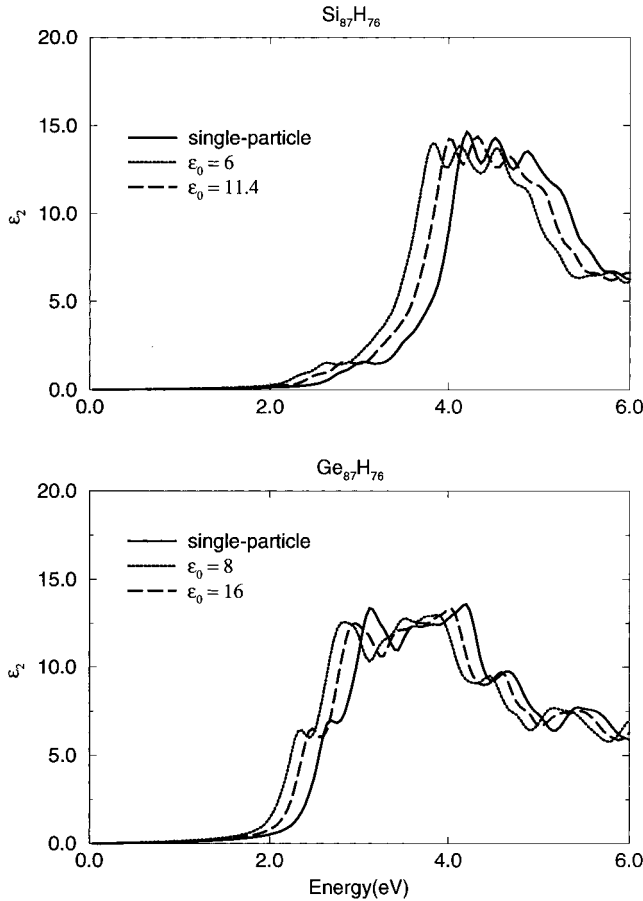


Fig. 7. Effects of the diagonal electron-hole Coulomb interaction in the optical spectra of Si and Ge dots of the same size. The effect of using different values for the dielectric constant is shown

### 3. Conclusions

Using the semi-empirical tight-binding approach we calculated the optical absorption spectra of some Ge nanocrystals. The theoretical single-particle spectra show a blue-shift of the  $E_1$  bulk peak, while we cannot make any prediction on the  $E_2$  peak, because the first-neighbour sp<sup>s</sup>\* parametrization has revealed not enough, for the germanium case, to describe it correctly. In order to explain the experimental results which present only a decrease of the intensity of the  $E_1$  peak with the decrease of the size and no blue-shift, we included, in a perturbative approach, the Coulomb electron–hole interaction. This induces a red-shift of the structures, but it is not able to explain the experimental results. In our opinion, differently from the first bound exciton state near the gap, where calculations within the perturbative approach give quite satisfactory results, in the case of the full optical spectrum, where a strong mixing of electron–hole couples can occur, a diagonalization of the full effective excitonic Hamiltonian cannot be avoided. A comparison with silicon dot spectra has been performed.

**Acknowledgements** This work has been supported in part by the Italian Ministero per l'Università e per la Ricerca Scientifica e Tecnologica (MURST-COFIN) and by the INFN Parallel Computing Initiative, using computer resources at the Interuniversity Consortium of the Northeastern Italy for Automatic Computing (CINECA).

### References

- [1] L.T. CANHAM, Appl. Phys. Lett. **57**, 1046 (1990).
- [2] Y. MAEDA, N. TSUKAMOTO, Y. YAZAWA, Y. KANEMITSU, and Y. MASUMOTO, Appl. Phys. Lett. **59**, 3168 (1991).
- [3] C.S. PENG, Q. HUANG, W.Q. CHENG, J.M. ZHOU, Y.H. ZHANG, T.T. SHENF, and C.H. TUNG, Phys. Rev. B **57**, 8805 (1998).
- [4] C.E. BOTTANI, C. MANTINI, P. MILANI, M. MANFREDINI, A. STELLA, P. TOGNINI, P. CHEYSSAC, and R. KOFMAN, Appl. Phys. Lett. **69**, 16 (1996).
- [5] S.H. KWOK, P.Y. YU, C.H. TUNG, Y.H. ZHANG, and M.F. LI, Phys. Rev. B **59** 4980 (1999).
- [6] P. TOGNINI, L.C. ANDREANI, M. GEDDO, A. STELLA, P. CHEYSSAC, R. KOFMAN, and A. MIGLIORI, Phys. Rev. B **53**, 6992 (1996).
- [7] S. OGUT, J.R. CHELIKOWSKY, and S. LOUIE, Phys. Rev. Lett. **79** (1997).
- [8] E. MARTIN, C. DELERUE, G. ALLAN, and M. LANNOO, Phys. Rev. B **50**, 18258 (1994).
- [9] L. WANG and A. ZUNGER, Phys. Rev. Lett. **77**, 1039 (1994).
- [10] P. VOGL, H.P. HJALMARSON, and J.D. DOW, J. Phys. Chem. Solids **44**, 365 (1983).
- [11] A. SELLONI and R. DEL SOLE, Surf. Science **168**, 35 (1986).
- [12] D.E. ASPNES and A.A. STUDNA, Phys. Rev. B **27**, 985 (1983).
- [13] G. CAPPELLINI, R. DEL SOLE, L. REINING, and F. BECHSTEDT, Phys. Rev. B **47**, 9892 (1993).
- [14] N.A. HILL and K.B. WHALEY, Phys. Rev. Lett. **75**, 1130 (1995).
- [15] A.B. CHEN and A. SHER, Phys. Rev. B **22**, 3886 (1980).
- [16] F. BECHSTEDT and R. DEL SOLE, Phys. Rev. B **38**, 7710 (1988).

